

IN THE UNITED STATES PATENT AND TRADEMARK OFFICE

Application of:	Young et al.	Confirmation No.:	3135
Serial No.:	10/657,363	Art Unit:	1648
Filed:	September 8, 2003	Examiner:	Hill, Myron G.
For:	ULTRA HIGH AFFINITY NEUTRALIZING ANTIBODIES	Attorney Docket No.:	10271-159-999 (CAM: 209073-999157)

DECLARATION OF DR. WILLIAM DALL'ACQUA UNDER 37 C.F.R. § 1.132

Commissioner for Patents
P.O. Box 1450
Alexandria, VA 22313-1450

Sir:

I, William Dall'Acqua, declare that:

1. I am presently an Associate Director at MedImmune, LLC ("MedImmune"), formerly MedImmune, Inc., the assignee of U.S. Serial No. 10/657,363 ("the '363 application").

2. I received my Ph.D. degree in Immunology from the University of Paris in Paris, France in 1996 under the supervision of Dr. Roberto Poljak and Dr. Graham Bentley. I received a Bachelor of Science degree in Biochemistry from the University of Paris in Paris, France in 1990. I have extensive experience with the engineering of immunoglobulin molecules. My academic, industrial and technical experience, as well as a list of my publications are set forth in my *curriculum vitae*, which is attached hereto as Exhibit 1.

3. I, or someone under my direction, prepared the RF-2 monoclonal antibody described in U.S. Patent No. 5,840,298 to Brams *et al.* ("Brams") in order to determine its *in vitro* microneutralization activity and binding parameters. In addition, I, or someone under my direction, investigated whether RF-2 and motavizumab (formerly known as Numax®)

monoclonal antibodies bind to identical sites on a respiratory syncytial virus ("RSV") F protein. The methodology used to generate the RF-2 antibody and results from the experiments conducted to determine the above activities are described below.

Synthesis, Expression and Purification of the RF-2 Monoclonal Antibody

4. In preparation for the synthesis of the variable regions of the RF-2 monoclonal antibody, I reviewed the sequence information provided in Brams. In my review, I noticed a number of inconsistencies in the variable heavy (VH) and variable light (VL) domain sequences (see, *e.g.*, Figures and Figure legend with respect to the RF-1 and RF-2 antibody sequences). For example, Figure 7b ("*RF1* VH domain") and Figure 11b ("*RF2* VH chain") have the same VH domain sequences; Figure 7b sequence is SEQ ID NO:15 ("*RF2* VH domain") in the Sequence Listing (not SEQ ID NO:13 ("*RF1* VH domain") as in Figure Legend); Figure 8b ("*RF2* VH domain") and Figure 9b ("*RF1* VH chain") have the same VH domain sequences; and Figure 8b sequence is SEQ ID NO:13 ("*RF1* VH domain") in the Sequence Listing (not SEQ ID NO:15 ("*RF2* VH domain") as in Figure Legend). Based on a careful review of the sequences, I chose to use the sequences provided in Figure 7b and Figure 8a of Brams for the VH and VL domains, respectively, of the RF-2 monoclonal antibody.

5. In a subsequent review of Heard *et al.* (1999) *Mol. Med.* 5:35-45 ("Heard"), a scientific article that describes the cloning and the recombinant production of the RF-2 monoclonal antibody, I confirmed the correct sequences of the RF-2 monoclonal antibody. The amino acid sequences in Figures 1 (bottom) and 2 (bottom) of Heard for the VH and VL domains of the RF-2 monoclonal antibody correspond to the amino acid sequences provided in Figure 7b and Figure 8a of Brams, respectively.

6. The variable light and variable heavy genes of the RF-2 monoclonal antibody were synthesized by GeneArt (Toronto, ON) and cloned into a mammalian expression vector encoding a human cytomegalovirus major immediate early (hCMVie) enhancer, promoter and 5'-untranslated region. In this system, a human $\gamma 1$ chain is secreted along with a human κ chain.

VH chain of monoclonal antibody RF-2

QVQLQESGPALVKPTQTLTLTCTFSGFSLSTRGMSVNWIRQPPGKALEWLARIDWDDDTFYASLKTRL
SISKDTSKNQVVL RMTNVD PVD TATYFCARASLYDSDSFYLFYHAYWGQGT VVT VSS

VL chain of monoclonal antibody RF-2

DIQMTQSPSSLSASVGDRVTITCRASQSIASYVNWYQQKPGKAPKVLIFASANLVSGVPSRFSGSGSGT
VFTLTISNLPEDFATYFCQQSYTNFSFGQGTKLEIK

7. Human Embryonic Kidney (HEK) 293 cells were transiently transfected with the antibody constructs using Lipofectamine (Invitrogen, Carlsbad, CA) and standard protocols. The secreted, soluble human IgG1 antibodies were purified from the conditioned media directly on 1 ml HiTrap protein A columns according to the manufacturer's instructions (GE Healthcare, Piscataway, NJ). Purified human IgG1s (typically >95 % homogeneity, as judged by SDS-polyacrylamide gels (PAGE) were dialyzed against Phosphate Buffered Saline (PBS), flash frozen and stored at -70°C.

RSV Microneutralization Assay

8. To assess the ability of the RF-2 monoclonal antibody to inhibit RSV replication *in vitro*, a standard RSV microneutralization assay was conducted. In addition to determining the microneutralization activity of the RF-2 monoclonal antibody, the microneutralization activities of other monoclonal antibodies specific for a RSV F protein (*i.e.*, palivizumab and motavizumab) as positive control antibodies and a negative control antibody (*i.e.*, R 347) were determined in parallel. Briefly, two-fold serial dilutions of palivizumab (Synagis®), motavizumab, RF-2 or R347 were made in duplicate in a 96-well plate. RSV A Long (ATCC, Manassas, VA) was then added to each well and incubated for 2 hours at 37°C in 5% CO₂. 2.5 x 10⁴ HEp-2 cells (ATCC, Manassas, VA) were then added to each well and incubated for 4 days at 37°C in 5% CO₂. Cells were then washed three times with PBS containing 0.1% Tween 20 and fixed with a cold mixture of 80% acetone/20% PBS. Viral replication was quantified by successive incubations with a mouse anti-RSV monoclonal antibody (Chemicon, Temecula, CA) and a horse radish peroxidase (HRP) conjugate of a goat anti-mouse IgG (Invitrogen, Carlsbad,

CA). Peroxidase activity was detected with 3,3',5,5'-tetramethylbenzidine (TMB) and the reaction was quenched with 2 M H₂SO₄. The absorbance was read at 450 nm and means plotted for each antibody concentration. The antibody concentrations that reduced viral replication to 50% when compared with virus-infected only (without antibody) control cells were then calculated and expressed as the IC₅₀.

9. Using the *in vitro* microneutralization assay, the IC₅₀ values for RF-2, Synagis®, and motavizumab were estimated at 11.7, 0.27 and 0.047 µg/ml, respectively (*see* Exhibit 2). Significantly higher amounts of the RF-2 monoclonal antibody were required to neutralize RSV by 50% as compared to Synagis® and motavizumab. In particular, a 43-fold higher amount of RF-2 monoclonal antibody was required to neutralize RSV by 50% as compared to Synagis®. A 249-fold higher amount of the RF-2 monoclonal antibody was required to neutralize RSV by 50% as compared to motavizumab. Accordingly, the RF-2 monoclonal antibody neutralizes RSV *in vitro*, but much higher concentrations are required as compared to Synagis® or motavizumab.

Binding Parameters

10. Using standard methodologies available to scientists as of at least 1999¹, the binding parameters for RF-2 monoclonal antibody and motavizumab binding to RSV F protein were determined. Briefly, the interaction of immobilized recombinant RSV F with soluble RF-2 and motavizumab was monitored using a KinExA 3000 instrument (Sapidyne Instruments, Boise, ID). Protein concentrations were calculated by the bicinchoninic acid (BCA) method. Generally, recombinant RSV F protein was coated onto azlactone beads at a concentration of 5 and 30 µg/ml in 0.05 M NaHCO₃, pH 9.0, for 1-2 days at 4°C according to manufacturer instructions (Sapidyne Instruments). Coated beads were then separated from unreacted recombinant RSV F using a gentle pulse spin and blocked for approximately 2 hours at room temperature with 1 M Tris, pH 8.0, bovine serum albumin 10 µg/ml. Beads were then resuspended in 30 ml of run buffer (PBS, pH 7.4 - 0.02% NaN₃) and secured into the instrument before use. Generally, each monoclonal antibody was prepared at concentrations of 2 and 40

¹ See, e.g., Blake *et al.* (1999) *Analytical Biochem.* 272:123, submitted herewith as Exhibit 4, which describes the KinEx A assay.

pM. Recombinant RSV F protein was then titrated across these monoclonal antibody concentration solutions at concentrations ranging from 0.00975-500 and 0.078-4000 pM and incubated for 2-6 days at room temperature to allow the mixtures to reach equilibrium. The mixtures were then injected over recombinant RSV F protein-coated bead packs, and the amount of free antibody in the samples was derived from the fluorescence signal obtained after the passing of Cy5-labeled goat anti-human IgG F(ab')₂ (typically 0.5 or 1 µg/ml; Jackson ImmunoResearch Laboratories, West Grove, PA) through the column. Dissociation constants (K_D) were determined by fitting the individual equilibrium titration data to a 1:1 binding model using the KinExA Pro 1.0.3. software.

11. In separate experiments, the association rates (k_{on}) for the interaction of the RF-2 monoclonal antibody and motavizumab with recombinant RSV F protein was determined by mixing each monoclonal antibody with recombinant RSV F protein, then detecting the amount of free antibody that remained as a function of time as the reaction approached equilibrium. More specifically, azlactone beads were pre-coated with recombinant RSV F protein at a concentration of 2 µg/mL as described above for the K_D determinations. For the actual k_{on} assessment, each monoclonal antibody was prepared at 100 pM, then mixed 1:1 with 100 pM of recombinant RSV F protein just prior to the start of the measurement. This resulted in starting concentrations in these mixtures of 50 pM antibody and 50 pM recombinant RSV F protein. The method used to detect free monoclonal antibody was similar to that described above for the K_D determinations, though the Cy5-labeled secondary reagent was used at a concentration of 0.75 µg/ml. Following each set of measurements, the data set was fit to obtain k_{on} using the KinExA Pro 1.0.3 software. The resulting k_{on} values for each monoclonal antibody was then used to calculate the corresponding dissociation rates (k_{off}) from the following relationship: $K_D = k_{off}/k_{on}$.

12. As shown in Exhibit 3, the K_D values for RF-2 and motavizumab are 737 fM and 420 fM, respectively. The affinity constants were then calculated ($K_a = 1/K_D$). The K_a for RF-2 is $1.36 \times 10^{12} \text{ M}^{-1}$ and the K_a for motavizumab is $2.38 \times 10^{12} \text{ M}^{-1}$.

RSV F Competition Assays


13. To determine whether or not the RF-2 monoclonal antibody and motavizumab bind to the same site of a RSV F protein, competition analysis of RF-2 and motavizumab for binding to RSV F protein was carried out using a BIAcore 3000 instrument (Uppsala, Sweden). The approach to these experiments was to attempt to saturate the epitope of one monoclonal antibody then immediately inject the second monoclonal antibody and look for additional binding. Briefly, recombinant RSV F protein was prepared at 100 nM in 10 mM NaOAc, pH4, and then immobilized at high density (784 RUs) onto a CM5 sensor chip using a standard amino coupling protocol as described by the instrument's manufacturer (BIAcore). Separately, a reference flow cell on the same sensor chip was prepared using the identical immobilization protocol, minus the protein. These two surfaces are connected in series, and the reference cell data is used to correct for any non-specific binding of the antibody injections, should it occur. Prior to the competition experiment, each monoclonal antibody was prepared at 3 and 6 μ M in instrument buffer (HBS-EP buffer containing 0.01 M HEPES, pH 7.4, 0.15 M NaCl, 3 mM EDTA and 0.005% P-20). The monoclonal antibody solutions were then injected either separately at 3 μ M, or co-injected after first pre-mixing the two 6 μ M solutions of monoclonal antibody at a 1:1 ratio (the resulting final concentration of each monoclonal antibody in the mixture thus equaled 3 μ M). Between injections, bound monoclonal antibody was removed from the recombinant RSV F protein surface using several pulses of 10 mM glycine buffer, pH 1.5.

14. Based upon the results from the competitive binding analysis, RF-2 binding to recombinant RSV F protein did not inhibit the binding of motavizumab to the same antigen (0% inhibition level; data not shown). Similarly, motavizumab binding to recombinant RSV F protein only minimally inhibited the binding of RF-2 to the same antigen (6% inhibition level; data not shown). Accordingly, these results seem to indicate that RF-2 and motavizumab do not bind to identical sites on a RSV F protein.

15. I hereby declare that all statements made herein of my own knowledge are true and that all statements made on information and belief are believed to be true; and further that

these statements were made with the knowledge that willful false statements and the like so made are punishable by fine or imprisonment, or both, under Section 1001 of Title 18 of the United States Code, and that such willful false statements may jeopardize the validity of the application or any patent issued thereon.

Date: June 16, 2008



William Dall'Acqua

EXHIBIT 1

***Curriculum Vitae* of Dr. William Dall'Acqua**

William F. Dall'Acqua, Ph.D.

Curriculum Vitae

PROFESSIONAL ADDRESS

MedImmune, LLC.
One MedImmune Way
Gaithersburg, MD 20878
Work: (301)398-4536
Fax: (301)398-9536
E-mail: dallacquaw@medimmune.com

PERSONAL ADDRESS

564 Chestertown Street
Gaithersburg, MD 20878
Home: (240)632-0291
Cell: (301)535-4756
E-mail: williamdallacqua@verizon.net

PERSONAL INFORMATIONS

Date and place of birth:	April 9, 1969, Paris, France
Citizenship:	French
Immigration status in USA:	Permanent Resident
Languages:	English and French

EDUCATION

1996: Ph.D. in Immunology with High Honors. University of Paris, France in conjunction with the University of Maryland.
1992: Pre-doctoral Thesis in Biochemistry with Highest Honors. University of Paris, France in conjunction with the Pasteur Institute.
1991: M.S. in Biochemistry with High Honors. University of Paris, France.
1990: B.S. in Biochemistry with High Honors. University of Paris, France.

HONORS AND AWARDS

1993-1996: Doctoral Fellowship from the French Department of Research.
1992: Pre-doctoral Achievement Award. Graduated first in my class.
1991: Pasteur Institute's pre-doctoral Fellowship.

PROFESSIONAL AFFILIATIONS

- Co-editor of one issue of Methods (Elsevier publication).

- Primary reviewer of a National Cancer Institute (NCI)/ National Institutes of Health (NIH) Site Review Team (03/17/04 to 03/19/04).
- Regular reviewer for the Journal of Immunology, the Journal of Molecular Biology, Trends in Immunology, Protein Engineering Design & Selection (PEDS), Clinical and Experimental Medicine and Drug Discovery Today.
- Invited speaker at Cambridge Healthtech Institute conferences (04/28/06; 05/16/07).
- Invited speaker at the Marcus Evans conference (10/04/07).
- Invited speaker at the US Patent and Trademark Office (08/23/06).
- Member of The American Society for Biochemistry and Molecular Biology (ASBMB), The American Society for Cell Biology (ASCB), The Society for Leukocyte Biology (SLB) and The American Association for the Advancement of Science (AAAS).

RESEARCH EXPERIENCE

04/05-present: Associate Director R&D, MedImmune, Inc., Department of Antibody Discovery and Protein Engineering, Gaithersburg, MD 20878.

- Led the antibody engineering group.
- Conceived and executed several novel protein engineering approaches.
- Engineered the interaction between immunoglobulins, antigens and Fc receptors.

01/02-04/05: Senior Scientist, MedImmune, Inc., Protein Engineering Department, Gaithersburg, MD 20878.

10/99-01/02: Scientist II, MedImmune, Inc., Immunology and Molecular Genetics Department, Gaithersburg, MD 20878.

02/97-10/99: Post-Doctoral Fellow, Molecular Oncology Department, Genentech, Inc., South San Francisco, CA 94080.

- Deciphered the contribution of domain interface residues to the stability of antibody C_H3 domain homodimers.
- Engineered the specificity of human neutrophil elastase.

09/93-09/96: Ph.D. Thesis research, Center for Advanced Research in Biotechnology (CARB), Rockville, MD 20850.

- Studied the molecular basis of various antigen-antibody interactions.

09/91-09/92: Pre-doctoral research training, Immunology Department, Pasteur Institute, Paris, France.

- Studied the interaction of lysozyme with anti-lysozyme antibodies and mutants thereof.

PROFESSIONAL SKILLS

Biochemistry/Biophysics/Structural Biology

- Extensive experience in protein purification/characterization, analysis of protein-protein interactions, protein crystallization and enzyme kinetic studies.
- Experienced in the analysis and modeling of the three-dimensional structure of proteins (PyMOL, Insight II, Midas, Swiss pdb Viewer and POV Ray).

Molecular Biology/Immunology:

- Proficient in most major aspects of molecular biology (gene cloning, mutagenesis, vector design, library construction) and immunological techniques (ADCC/CDC assays, ELISA, FACS, IP and related assays).
- Successfully expressed numerous recombinant proteins in E. Coli, yeast and mammalian cells.
- Experienced in the construction and screening of phage peptide or antibody libraries as well as in the generation of monoclonal antibodies using the hybridoma technology.

Legal/Regulatory:

- Extensive knowledge of the Intellectual Property issues surrounding the protein engineering field.
- Experienced in the preparation of patent applications, pre-IND and IND packages.

SCIENTIFIC PUBLICATIONS

Dall'Acqua, W¹, and Wu, H. (2008). Modulation of serum proteins homeostasis and transcytosis by the neonatal Fc receptor. In Therapeutic Antibodies: from Theory to Practice. John Wiley & Sons publishers. In press. ¹*Corresponding author*.

Oganesyan, V., Gao, C., Shirinian, L., Wu, H. and Dall'Acqua, W¹. (2008). Structural Characterization of a Human Fc Fragment Engineered for Lack of Effector Functions. Acta Crystallogr. Sect. D. D64, 700-704. ¹*Corresponding author*.

Oganesyan, V., Damschroder, M., Leach, W., Wu, H. and Dall'Acqua, W¹. (2008). Structural Characterization of a Mutated, ADCC-Enhanced Human Fc Fragment. Mol. Immunol. 45, 1872-1882. ¹*Corresponding author*.

Damschroder, M., Widjaja, L., Gill, P.S., Krasnoperov, V., Jiang, W., Dall'Acqua, W¹, and Wu, H. (2007). Framework Shuffling of Antibodies to Reduce Immunogenicity and Manipulate Functional and Biophysical Properties. Mol. Immunol. 44, 3049-3060. ¹*Corresponding author*.

Dall'Acqua, W¹, Kiener, P.A. and Wu, H. (2006). Properties of Human IgG1s Engineered for Enhanced Binding to FcRn. J. Biol. Chem. 281, 23514-23524. ¹*Corresponding author*.

Dall'Acqua, W¹, Cook, K., Damschroder, M., Woods, R. and Wu, H. (2006). Modulation of the Effector Functions of a Human IgG1 through Engineering of its Hinge Region. J. Immunol. 177, 1129-1138. ¹*Corresponding author*.

Wu, H. and Dall'Acqua, W¹. (2005). Editorial: Humanized Antibodies and Their Applications. Methods 36, 1-2. ¹*Corresponding author*.

Dall'Acqua, W¹, Damschroder, M., Zhang, J., Widjaja, L., Yu, G. and Wu, H. (2005). Humanization of Antibodies by Framework Shuffling. Methods 36, 43-60. ¹*Corresponding author*.

Damschroder, M.M, Kozhich, A., Woods, R.M., Cheng, L., Mullikin, B.A., Wilson, S.D., Ulbrandt, N.D., Bachy, C.M., Wu, H., Suzich, J.A., Kiener, P.A., Dall'Acqua, W¹, and White, W.I. (2004). Analysis of Human and Primate CD2 Molecules by Protein Sequence and Epitope Mapping with Anti-Human CD2 Antibodies. Mol. Immunol. 41, 985-1000. ¹*Corresponding author*.

Dall'Acqua, W¹, Woods, R., Ward, S., Palaszynski, S., Patel, N.K., Brewah, Y., Wu, H., Kiener, P.A. and Langermann, S. (2002). Increasing the Affinity of a Human IgG1 for the Neonatal Fc Receptor: Biological Consequences. J. Immunol. 169, 5171-5180. ¹*Corresponding author*.

Dall'Acqua, W. and Carter, P. (2000). Substrate-Assisted Catalysis: Molecular Basis and Biological Significance. *Protein Sci.* 9, 1-9.

Dall'Acqua, W., Halin, C., Rodrigues, M.L. and Carter, P. (1999). Human Neutrophil Elastase Substrate Specificity Tailored Through 'Substrate-Assisted Catalysis' and Substrate Phage. *Protein Eng.* 12, 981-987.

Dall'Acqua, W. and Carter, P. (1998). Antibody Engineering. *Curr. Opin. Struct. Biol.* 8, 443-450.

Dall'Acqua, W., Simon, A., Mulkerrin, M.G. and Carter, P. (1998). Contribution of Domain Interface Residues to the Stability of Antibody C_H3 Domain Homodimers. *Biochemistry* 37, 9266-9273.

Dall'Acqua, W., Goldman, E.R., Lin, W., Teng, C., Daisuke, T., Li, H., Ysern, X., Braden, B.C, Li, Y., Smith-Gill, S.J. and Mariuzza, R.A. (1998). A Mutational Analysis of Binding Interactions in an Antigen-Antibody Protein-Protein Complex. *Biochemistry* 37, 7981-7991.

Goldbaum, F.A., Velikovsky, C.A., Dall'Acqua, W., Fossati, C.A., Fields, B.A., Braden, B.C, Poljak, R.J. and Mariuzza, R.A. (1997). Characterization of Anti-Anti-Idiotypic Antibodies that Bind Antigen and an Anti-Idiotypic. *Proc. Natl. Acad. Sci. USA.* 94, 8697-8701.

Goldman, E.R., Dall'Acqua, W., Braden, B.C. and Mariuzza, R.A. (1997). Analysis of Binding Interactions in an Idiotope-Anti-Idiotope Protein-Protein Complex by Double Mutant Cycles. *Biochemistry* 36, 49-56.

Fields, B.A, Goldbaum, F.A., Dall'Acqua, W., Malchiodi, E.L., Cauerhff, A., Schwarz, F.P., Ysern, X., Poljak, R.J. and Mariuzza, R.A. (1996). Hydrogen Bonding and Solvent Structure in an Antigen-Antibody Interface. Crystal Structures and Thermodynamic Characterization of Three Fv Mutants Complexed with Lysozyme. *Biochemistry* 35, 15494-15503.

Braden, B.C., Fields, B.A., Ysern, X., Dall'Acqua, W., Goldbaum, F.A., Poljak, R.J. and Mariuzza, R.A. (1996). Crystal Structure of an Fv-Fv Idiotope-Anti-Idiotope Complex at 1.9Å Resolution. *J. Mol. Biol.* 264, 137-151.

Dall'Acqua, W., Goldman, E.R., Eisenstein, E. and Mariuzza, R.A. (1996). A Mutational Analysis of the Binding of Two Different Proteins to the Same Antibody. *Biochemistry* 35, 9667-9676.

Braden, B.C., Fields, B.A., Ysern, X., Goldbaum, F.A., Dall'Acqua, W., Schwarz, F.P., Poljak, R.J. and Mariuzza, R.A. (1996). Crystal Structure of the Complex of the Variable

Domain of Antibody D1.3 and Turkey Egg-White Lysozyme: a Novel Conformational Change in Antibody CDR-L3 Selects for Antigen. *J. Mol. Biol.* 257, 889-894.

Braden, B.C., Dall'Acqua, W., Eisenstein, E., Fields, B.A., Goldbaum, F.A., Malchiodi, E.L., Mariuzza, R.A., Poljak, R.J., Schwarz, F.P., Ysern, X. and Poljak, R.J. (1995). Protein Motion and Key Complementarity in Antigen-Antibody Reactions. *Pharm. Acta Helv.* 69, 225-230.

Braden, B.C., Cauerhff, A., Dall'Acqua, W., Fields, B.A., Goldbaum, F.A., Malchiodi, E.L., Mariuzza, R.A., Poljak, R.J., Schwarz, F.P., Ysern, X. and Bhat, T.N. (1995). Structure and Thermodynamics of Antigen Recognition by Antibodies. *Annals of the New York Academy of Sciences* 764, 315-327.

Ysern, X., Fields, B.A., Bhat, T.N., Goldbaum, F.A., Dall'Acqua, W., Schwarz, F.P., Poljak, R.J. and Mariuzza, R.A. (1994). Solvent Rearrangement in an Antigen-Antibody Interface Introduced by Site-Directed Mutagenesis of the Antibody Combining Site. *J. Mol. Biol.* 238, 496-500.

Bhat, T.N., Bentley, G.A., Boulot, G., Greene, M.I., Tello, D., Dall'Acqua, W., Souchon, H., Schwarz, F.P., Mariuzza, R.A. and Poljak, R.J. (1994). Bound Water Molecules and Conformational Stabilization Help Mediate an Antigen-Antibody Association. *Proc. Natl. Acad. Sci. USA.* 91, 1089-1093.

ISSUED PATENTS

Dall'Acqua, W., Johnson, S. and Ward, S. (2006). Molecules with extended half-lives, compositions and uses thereof. US patent number 7,083,784.

Reed, J., Dall'acqua, W., Van Snick, J., Renauld, J.C., Cormont, F. and Uyttenhove, C. (2008). Recombinant anti-interleukin-9 antibodies. US patent number 7,371,383.

PUBLISHED PATENTS

Dall'Acqua, W. and Wu, H. Molecules with reduced half-lives, compositions and uses thereof. Publication number WO08048545A2 (2008).

Damschroder, M., Dall'Acqua, W., Wu, H. and Bowden, E. Humanized anti-EphB4 antibodies and their use in treatment of oncology and vasculogenesis-related disease. Publication number WO08042941A2 (2008).

Damschroder, M., Kiener, P., Wu, H., Dall'Acqua, W., Herbst, R. and Coyle, A. Humanized anti-CD19 antibodies and their use in treatment of oncology, transplantation and autoimmune disease. Publication number WO08031056A2 (2008).

Damschroder, M., Dall'Acqua, W., Wu, H. and Kinch, M. Affinity optimized EphA2 agonistic antibodies and methods of use thereof. Publication number WO2007075706A2 (2007).

Wellstein, A., Bowden, E., Tassi, E., Tice, D., Dall'Acqua, W., Wu, H., Gao, C., Coats, S. and Gao, J. ALK antagonist, agonist, and uses thereof. Publication number WO2007059300A2 (2007).

Allan, C., Wu, H., Swers, J. and Dall'Acqua, W. An integrated approach for generating multidomain protein therapeutics. Publication number WO2007005612A2 (2007). European application number EP1899477A2 (2008).

Dall'Acqua, W., Wu, H., Damschroder, M. and Casas-Finet, J. Modulation of antibody effector functions by hinge domain engineering. Publication number WO2006116260A2 (2006). European application number EP1874816A2 (2008).

Wu, H., Dall'Acqua, W. and Damschroder, M. Framework shuffling of antibodies. Publication numbers US20060228350A1 (2006) and WO2006102095A2 (2006). European application number EP1869192A2 (2007).

Losonky, G., Connor, E.M., Young, J.F., Wu, H. and Dall'Acqua, W. Methods of preventing and treating RSV infections and related conditions. Publication numbers US20060115485A1 (2006) and WO2006050166A2 (2006). European application number EP1812068A2 (2007).

Dall'Acqua, W., Kinch, M. and Carles-Kinch, K. Modulation of antibody specificity by tailoring the affinity to cognate antigens. Publication numbers US20060121042A1 (2006) and WO2006047639A2 (2006). European application number EP1809326A2 (2007).

Dall'Acqua, W., Wu, H. and Damschroder, M. Increasing the production of recombinant antibodies in mammalian cells by site-directed mutagenesis. Publication numbers US20060019342A1 (2006) and WO2006004663A2 (2006). European application number EP1773391A2 (2007).

Dall'Acqua, W., Wu, H. and Damschroder, M. Periplasmic expression of antibodies using a single signal sequence. Publication numbers US20050181479A1 (2005) and WO06093496A1 (2006). European application number EP1856137A1 (2007).

Wu, H., Dall'Acqua, W. and Damschroder, M. Humanization of antibodies. Publication numbers US20050048617A1 (2005) and WO05042743A2 (2005). European application number EP1660186A2 (2006).

Wu, H., Dall'Acqua, W. and Damschroder, M. Humanization of antibodies. Publication numbers US20050042664A1 (2005) and WO05035575A2 (2005). European application number EP1660534A2 (2006).

Reed, J., Dall'acqua, W., Van Snick, J., Renauld, J.C., Cormont, F. and Uyttenhove, C. Recombinant anti-interleukin-9 antibodies. Publication number WO03086458A1 (2003). European application numbers EP1499352A1 (2005).

Carter, P., Dall'Acqua, W. and Rodrigues, M. Elastase variants and substrates. Publication number WO0068363A2 (2000).

FILED PATENTS

Dall'Acqua, W., Oganessian, V. and Wu, H. (2007). Crystals and structure of a human Fc variant.

Damschroder, M., Kiener, P., Wu, H. and Dall'Acqua, W. (2006). Humanized anti-CD19 antibodies and their use in treatment of oncology, transplantation and autoimmune disease.

NEW GENES AND STRUCTURES SUBMISSIONS

Dall'Acqua, W. (2003). Pan troglodytes (chimpanzee), Macaca fascicularis (cynomolgus monkey), Macaca mulatta (rhesus monkey), Macaca nemestrina (pig-tailed macaque), Macaca arctoides (stumped-tailed macaque), Papio anubis (olive baboon), Cercocebus torquatus atys (african green monkey) and Macaca assamensis (assamese macaque) cluster of differentiation 2 (CD2). GenBank accession numbers AY445034, AY445036, AY445037, AY445041, AY445040, AY445035, AY445038 and AY445039, respectively.

Oganessian, V., Wu, H. and Dall'Acqua, W. (2007). Structural Characterization of a Mutated, ADCC-Enhanced Human Fc Fragment. PDB accession number 2QL1.

Oganessian, V., Wu, H. and Dall'Acqua, W. (2008). Structural Characterization of a Human Fc Fragment Engineered for Lack of Effector Functions. PDB accession number 3C2S.

EXHIBIT 2

A₄₅₀

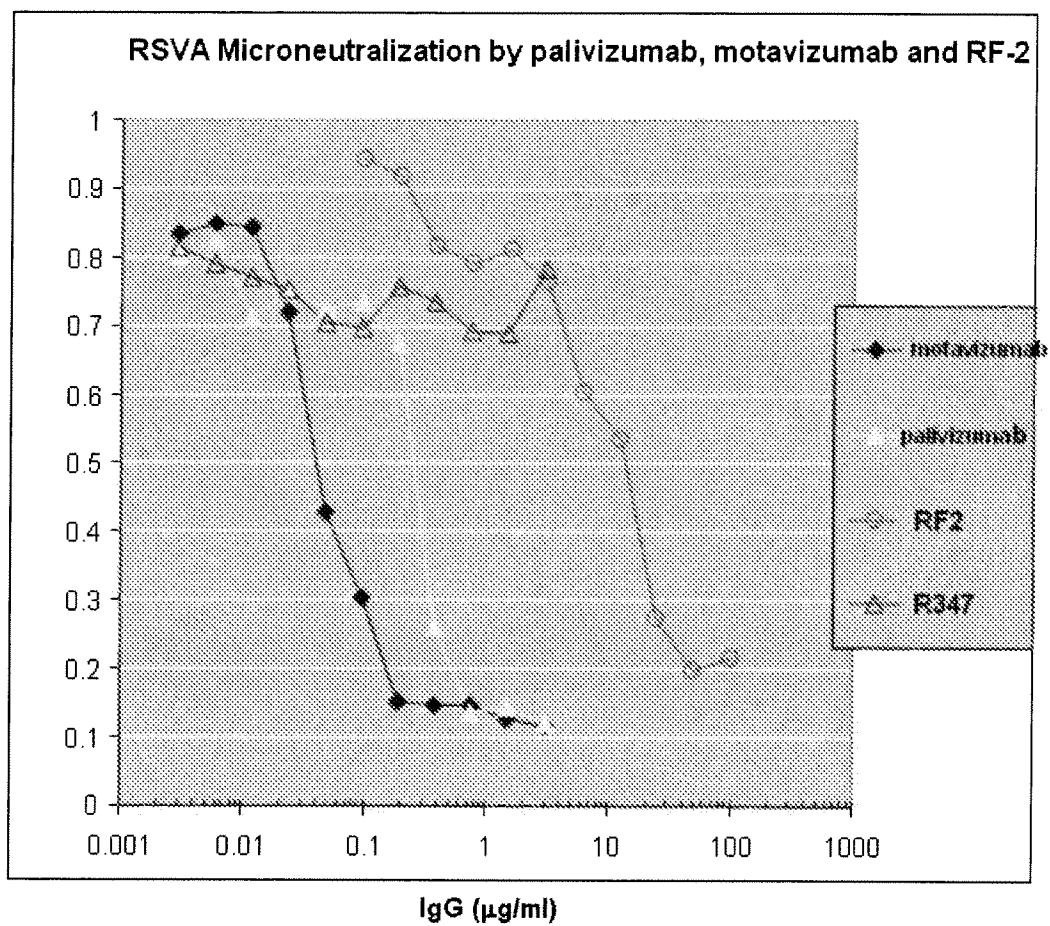


EXHIBIT 3

IgG	k_{on} (1/M.s)	k_{off} (1/s)	K_D (fM)
Numax™	8.20e+5	3.45e-7	420
RF-2	8.25e+5	6.08e-7	737

EXHIBIT 4

Blake *et al.* (1999) *Analytical Biochem.* 272:123

Automated Kinetic Exclusion Assays to Quantify Protein Binding Interactions in Homogeneous Solution

Robert C. Blake II,^{*,1} Andrey R. Pavlov,[†] and Diane A. Blake[†]

College of Pharmacy, Xavier University, 7325 Palmetto Street, New Orleans, Louisiana 70125; and [†]Department of Ophthalmology, Tulane University School of Medicine, 1430 Tulane Avenue, New Orleans, Louisiana 70112

Received December 15, 1998

A method was developed for the quantification of protein-ligand interactions in which the free protein present in homogeneous reaction mixtures was separated and quantified using a KinExA immunoassay instrument. Separation was achieved by rapid percolation of the reaction mixture over a column of microbeads whose surfaces were coated with an immobilized form of the ligand. The protein thus captured was quantified using a fluorescently labeled anti-protein antibody. The features of this new method were illustrated using a model system in which each of the principal reagents was covalently labeled with a different fluorescent molecule: mouse monoclonal anti-biotin primary antibody (fluorescein), biotin (B-phycoerythrin), and goat anti-mouse polyclonal secondary antibody (indodicarbocyanin). Values for the equilibrium and kinetic rate constants for the binding between the anti-biotin antibody and biotin conjugated with B-phycoerythrin were determined and shown to be independent of whether the fluorescent label was located on the primary or secondary antibody. Equilibrium binding experiments conducted with $(F_{AB})_2$ and corresponding F_{AB} fragments showed that the valency of the binding protein had no influence on the value of the dissociation constant. The values of the equilibrium and rate constants obtained by this new method are those for the binding reaction in homogeneous solution; the immobilized ligand is only a tool exploited for the separation and quantification of the free protein. © 1999 Academic Press

The interaction of proteins with small ligands and other biopolymers has been the subject of extensive theoretical and experimental research for decades (1–

5). Methods for the quantification of protein binding interactions may be arbitrarily divided into two categories, homogeneous and heterogeneous. Homogeneous methods are those where all of the binding reagents are evenly dispersed in solution. These methods require that some quantifiable property of the binding partners be changed as a consequence of the interaction; examples include absorbance, fluorescence, fluorescence polarization, and sedimentation coefficient. A variety of homogeneous methods are available to quantify protein interactions that exhibit equilibrium dissociation constants in the μM or higher range (see 4 and references therein).

A number of heterogeneous methods have also been described for the quantification of high affinity binding interactions (6–8). A heterogeneous method is defined herein as one in which one or more of the binding reagents is immobilized on a surface. With the introduction of a commercial surface plasmon resonance (SPR)² biosensor early in this decade (9–11), optical evanescent wave biosensors have become increasingly popular as a tool for the qualitative and quantitative characterization of reversible interactions among biological macromolecules. These biosensors exploit refractive index changes to detect specific reversible binding of a reactant in a mobile phase to a binding partner immobilized on the surface of the sensor. Despite the popularity of the commercial SPR biosensors, there is a growing uneasiness regarding the validity of both the rate and equilibrium data derived from these methods (12). Investigators have expressed concerns about the problems of limiting mass transport to the immobile binding phase (13–15), immobilization in multiple conformations (16–18), steric hindrance on

¹ To whom correspondence should be addressed. Fax: 504-485-7930. E-mail: rblake@xula.edu.

² Abbreviations used: SPR, surface plasmon resonance; HBS, Hepes buffer saline, 137 mM NaCl, 3.0 mM KCl, 10 mM sodium 2-hydroxyethylpiperazine-*N*'-2-ethanesulfonate, pH 7.4; BSA, bovine serum albumin; Cy5, indodicarbocyanine dye.

the surface (19), the widespread use of data subset analysis (16, 20, 21), the reported lack of self-consistency (16, 22–25), and the inappropriate use of a simple 1:1 pseudo-first-order description for binding of multivalent mobile or immobile reactants (16, 26–28).

This paper describes a new method to study protein binding interactions where the immobilized binding partner is merely a tool used to capture and quantify a portion of the free, uncomplexed protein present in homogeneous solution reaction mixtures. Homogeneous mixtures of protein, ligand, and protein–ligand complexes were briefly exposed to an immobilized derivative of the ligand to permit a subset of those protein molecules in the mixture with unoccupied binding sites to be captured and retained on the solid phase. The time of exposure to the immobilized ligand was kept sufficiently brief to ensure that negligible dissociation of soluble protein–ligand complexes could occur. Those protein molecules in solution that were already complexed with the soluble ligand were thus kinetically excluded from binding to the ligand on the immobile phase. The amount of free protein thus captured was quantified using a fluorescently labeled antibody directed against the captured protein. The operating principles of this method were illustrated using a model system where all of the principal reagents were covalently labeled with different fluorescent molecules. Both equilibrium binding and kinetic rate constants were determined for individual protein binding interactions. Unlike other heterogeneous methods, the assays described herein yielded data for binding interactions between soluble partners in homogeneous solution.

MATERIALS AND METHODS

Materials. Fluorescein-labeled mouse anti-biotin monoclonal and fluorescein-labeled and indodicarbocyanine (Cy5)-labeled goat anti-mouse polyclonal antibodies were obtained from Jackson ImmunoResearch Laboratories, Inc. (West Grove, PA). Mouse anti-digoxin monoclonal antibody (clone number 94146) and the digoxin–bovine serum albumin (BSA) covalent conjugate were obtained from Fitzgerald Industries International, Inc. (Concord, MA). Fluorescein thiocarbamylethylenediamine coupled via an (*O*-carboxymethyl)oxime linkage to a dialdehyde derivative of digoxin in the terminal sugar residue was purchased from The Binding Site, Inc. (San Diego, CA). The biotin–BSA conjugate and the biotinylated B-phycoerythrin (5 mol of biotin/mol protein) were purchased from Sigma Chemical Co. (St. Louis, MO). Isoton II was obtained from Fisher Scientific (Houston, TX). All other chemicals were reagent grade. Polymethylmethacrylate beads were the “98- μm ” fraction obtained from Bangs Laboratories, Inc. (Carmel, IN). The fluo-

rescein, B-phycoerythrin, and Cy5 optical filter sets for the KinExA were obtained from Sapidyn Instruments, Inc. (Boise, ID).

Preparation of antibody fragments. Fragments of mouse monoclonal anti-digoxin antibody were prepared using the ImmunoPure IgG1 F_{AB} and (F_{AB})₂ Preparation Kit from Pierce Chemical Co. (Rockford, IL). Briefly, separate samples of the intact antibody were subjected to limited proteolytic cleavage with immobilized ficin, followed by removal of undigested IgG1 and F_C fragments by passage of the reaction products through a column of immobilized protein A. The activity of the immobilized ficin and the reduction of disulfide binds in the antibody was purposefully controlled by varying the concentration of cysteine activator as described in the manufacturer's printed instructions. The final yields recovered from the preparation of (F_{AB})₂ and F_{AB} were 18.5 and 34.8%, respectively, of the initial IgG1.

Equilibrium and kinetic binding measurements. Equilibrium and kinetic measurements of antibody–antigen binding interactions were performed with a beta unit of the KinExA 3000 immunoassay instrument (Sapidyn Instruments, Inc.). Binding studies were conducted in two experimental systems: biotinylated B-phycoerythrin binding to anti-biotin antibody and fluorescein-labeled digoxin binding to anti-digoxin antibody. For either equilibrium or kinetic studies, polymethylmethacrylate beads (140–170 mesh, 98 μm) were coated with antigen by suspending 200 mg (dry wt) of beads in 1.0 ml Hepes-buffered saline (137 mM NaCl, 3.0 mM KCl, 10 mM sodium 2-hydroxyethylpiperazine-*N*'-2-ethanesulfonate, pH 7.4, HBS) that contained 100 μg of either a biotin–BSA or a digoxin–BSA conjugate. After 1 h of gentle agitation at 37°C, the beads were centrifuged, and the supernatant solution was decanted. Nonspecific protein binding sites that remained on the beads were blocked by the subsequent incubation of the beads with 1.0 ml of 10% (w/v) goat serum in HBS that contained 0.03% NaN₃ for an additional hour at 37°C. The blocked beads were stored at 4°C in the blocking solution for up to a month before use.

A beadpack approximately 4 mm high was created in the observation cell of the KinExA by drawing 675 μl of a suspension of the blocked beads in HBS (6.5 mg beads/ml) over the retention screen at a flow rate of 1.5 ml/min and washing the retained beads with sufficient HBS buffer (1.0 ml) to remove the excess goat serum. The beads were then gently disrupted with a brief backflush of HBS (50 μl at 300 $\mu\text{l}/\text{min}$), followed by a 20-s settling period to create a uniform and reproducible pack.

For equilibrium measurements, each monoclonal antibody was incubated with different concentrations of

its corresponding antigen. BSA was present at 0.5 mg/ml in the reaction mixtures to reduce subsequent nonspecific binding of the primary antibody in the instrument. Once equilibrium was achieved (less than 10 min in all cases), 500 μ l of the mixture was drawn past the beads, followed by 800 μ l of the HBS buffer to wash out unbound primary antibody and excess soluble antigen. One milliliter of fluorescently labeled goat anti-mouse antibody containing 1.0 mg/ml BSA was then drawn past the beads. All solution transfers up to this point were accomplished with a flow rate of 500 μ l/min. Unbound labeled secondary antibody was subsequently removed by drawing 3.0 ml of HBS through the beadpack over a period of 2 min.

For kinetic measurements, equal volumes (250 μ l) of the primary antibody and soluble antigen solutions were mixed at rates of 250 μ l/min each. The binding reaction proceeded for the 7 s it took the mixture to transverse the distance from the point of mixing to the point where the beadpack was first encountered. One milliliter of labeled secondary antibody was then drawn past the beads (at 500 μ l/min), followed by 1.5 ml (at 750 μ l/min) of HBS.

Data acquisition (initiated in all cases immediately following the establishment of the microcolumn of packed beads) and instrument control were accomplished via an IBM personal computer interfaced to the KinExA using software provided by Sapidyne Instruments, Inc. Data analysis was accomplished by importing the KinExA data into SlideWrite (version 2.1, Advanced Graphics, Inc., Carlsbad, CA) and exploiting various linear and nonlinear regression curve-fitting routines contained therein.

Electrical impedance measurements. Absolute numbers of individual beads were determined by particle counting in a Multisizer IIe (Coulter Scientific Instruments, Inc., Hialeah, FL) fitted with a 280- μ m aperture. The instrument was programmed to siphon 2.0 ml of sample volume. The sample consisted of 200 mg (dry wt) of blocked polymethylmethacrylate beads in 1.0 ml of 10% (w/v) goat serum suspended in 90 ml of Isoton II as the electrolyte. The current applied across the aperture was 3.2 mA. Voltage pulses attendant with impedance changes as particles passed through the aperture were monitored with an instrument gain of 4.

RESULTS

KinExA assays quantify free protein. A beta unit of the KinExA 3000 instrument was used to quantify protein binding interactions. The KinExA instrument is a computer-controlled flow spectrofluorimeter designed to achieve the rapid separation and quantification of free, unbound protein present in reaction mixtures of free protein, free ligand, and protein-ligand

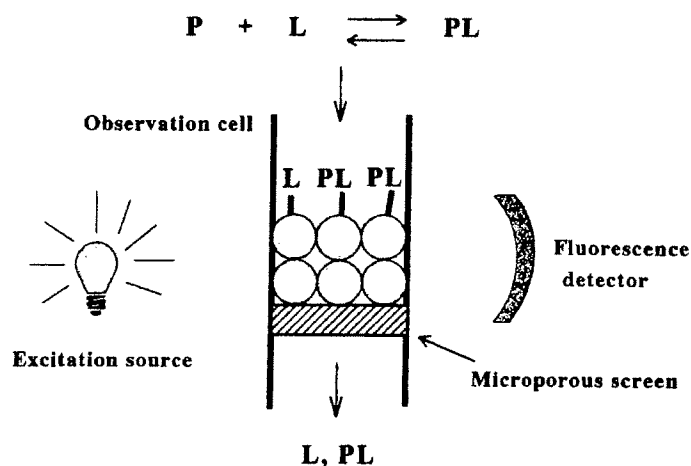


FIG. 1. Schematic of KinExA immunoassay instrument. P, L, and PL represent free protein, free ligand, and protein-ligand complex, respectively.

complexes. The operating principles of the instrument are illustrated schematically in Fig. 1. Briefly, the KinExA consists of a capillary flow/observation cell (inner diameter = 1.6 mm) fitted with a microporous screen through which various solutions are drawn under negative pressure. Uniform particles larger than the average pore size of the screen (53 μ m) are precoated with ligand and deposited above the screen in a packed bed. A small volume of the reaction mixture, typically 0.5 ml, is then percolated through the packed bed of ligand-coated microbeads under negative pressure. Proteins with unoccupied ligand binding sites are available to bind to the immobilized ligand coated on the surface of the microbeads; proteins with binding sites occupied by soluble ligand are not. Exposure of the soluble protein-ligand complex to the immobilized ligand is sufficiently brief (~480 ms for a flow rate of 0.5 ml/min) to ensure that negligible dissociation of the soluble complex occurs during the time of exposure to the beads. Those proteins whose binding sites are occupied by ligands with slow unimolecular dissociation rate constants are thus kinetically excluded from interacting with the immobilized ligand. The soluble reagents are removed from the beads by an immediate buffer wash. Quantification of the protein thus captured on the immobilized ligand can subsequently be achieved by the brief exposure of the particles to a fluorescently labeled antibody directed against the protein, followed by measurement of the resulting fluorescence from the particles after removal of excess unbound reagents.

Effect of antibody concentration on the instrument response. The ability of the KinExA to quantify proteins with unoccupied binding sites was assessed in an experimental system comprised of an anti-biotin monoclonal antibody and biotinylated BSA absorption-coated onto polymethylmethacrylate beads. Figure 2

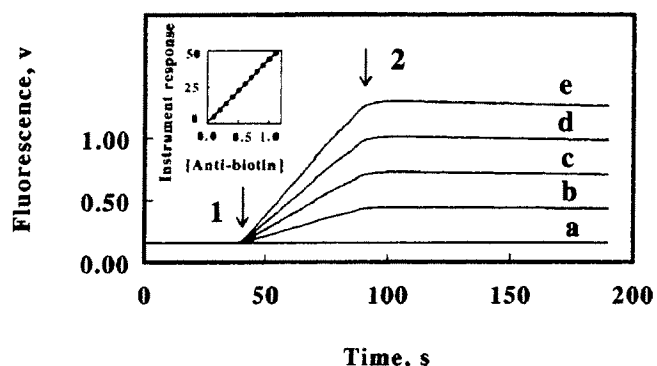


FIG. 2. Capture, retention, and quantification of free protein using the KinExA. Main panel, time courses of individual fluorescence responses in the KinExA instrument when beads coated with biotinylated BSA were exposed to different concentrations of a fluorescein-labeled mouse anti-biotin monoclonal antibody. Concentrations of anti-biotin binding sites were zero, 0.2, 0.4, 0.6, and 0.8 nM in experiments a through e, respectively. Arrows: 1, introduction of fluorescein-labeled anti-biotin; and 2, cessation of anti-biotin and initiation of buffer wash. Inset, standard curve of free anti-biotin captured and retained on the beads bearing biotinylated BSA at low concentrations of the soluble anti-biotin antibody. The value of the instrument response represents the integrals of individual time courses from 100 to 190 s; each datum was collected in triplicate.

shows typical time courses for the fluorescence signal when different concentrations of a fluorescein-labeled anti-biotin monoclonal antibody were analyzed in the KinExA in the absence of soluble biotin or biotin derivatives. The fluorescence signal from zero to 40 s corresponded to the background signal generated while buffer alone passed through the packed column of microbeads. The beads coated with biotinylated BSA were then exposed to different solutions of fluorescein-labeled antibiotin (40 to 90 s), followed by a buffer wash to remove any excess unbound antibody (90 to 190 s). It was evident that (i) very little of the fluorescein-labeled antibody captured and retained on the beads was removed during the buffer wash and (ii) the higher the concentration of antibiotin in the sample, the higher was the corresponding fluorescence signal.

The instrument response as a function of the concentration of labeled antibiotin is shown in the inset of Fig. 2. The instrument response was taken as the integrated fluorescence signal over the last 90 s of the experimental trace (the 100- to 190-s interval for curves such as those in Fig. 2). The instrument response was approximately linear with the concentration of antibody binding sites up to 1.0 nM. Beyond that concentration (up to 13 nM, data not shown), the data were approximated by a rectangular hyperbola with a maximal value of 760 V-s at an infinite concentration of binding sites and a half-maximal response at 16 nM in binding sites. Under normal operating conditions, binding experiments with the KinExA are conducted with 0.5 to 3.0 nM antibody; thus only a small fraction of the ligand in the beadpack is involved in

antibody binding under the experimental conditions used for routine equilibrium and kinetic rate constant determinations.

The fluorescence signal observed from the beadpack was proportional to the absolute amount of captured fluorescein-labeled antibody. To determine the proportionality constant, the observation cell was repositioned such that the contents of the capillary tube were viewed downstream from the microporous screen, after the solution had passed through the beadpack. Curve a in Fig. 3A shows the time course of the fluorescence signal when 0.5 ml of 2.4 nM (in binding sites) fluorescein-labeled antibiotin was drawn through the obser-

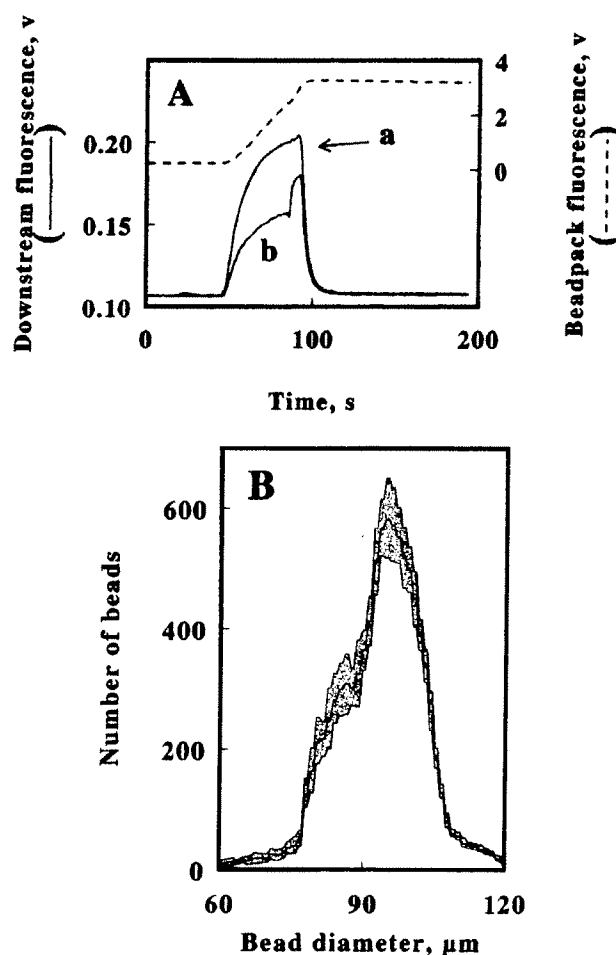


FIG. 3. Determination of the number of antibody binding sites in the standard KinExA beadpack. (A) Time courses of the fluorescence responses viewed from the beadpack (dashed line) or downstream from the beadpack (solid lines) when 2.4 nM fluorescein-labeled anti-biotin was drawn through the observation cell in the absence (a) and presence (b) of beads coated with biotinylated BSA. (B) Electrical impedance measurements of the absolute number of beads as a function of particle diameter for the coated spherical beads employed in the KinExA. The volume of bead suspension drawn through the aperture of the Multisizer IIe corresponded to 99% of that drawn through the observation cell of the KinExA per experiment. The data points and the shaded area represent the mean and standard deviation, respectively, of 14 determinations.

vation cell in the absence of beads. The excursion of the kinetic trace from the baseline between 40 and 100 s represents the total fluorescence observed at that flow rate for 1.2 pmol of binding sites ($0.5 \text{ ml} \times 2.4 \text{ nM}$). Curve b in Fig. 3A shows the time course of the fluorescence signal for the same experiment conducted with a 4-mm column of beads bearing biotinylated BSA retained upstream of the microporous screen. The decrease in the total fluorescence signal of curve b relative to that of curve a over the interval of 40 to 100 s (42% or 0.5 pmol) was taken to represent the percentage of antibody that was captured and retained in the beadpack. The 42% capture efficiency noted here appears to be unusually high; analogous experiments with other binding partners indicate that a more typical capture efficiency is less than 10% of the soluble free protein (data not shown). The dashed curve in Fig. 3A shows the time course of the fluorescence signal for the same experiment as observed from directly opposite the column of packed beads. Thus, when integrated from 100 to 190 s, this signal (98 V-s) corresponded to the 0.5 pmol of fluorescent antibody bound to the beadpack and was equivalent to 12.9% of the total extrapolated maximal signal at an infinite antibody concentration. Thus the maximal binding capacity of a 4-mm beadpack coated with biotinylated BSA was calculated to be 3.9 pmol of binding sites.

The size distribution of the microbeads used in this study is given in Fig. 3B. The solid mean line in Fig. 3B is a step function of absolute counts as a function of particle size, determined on the Multisizer IIe with a suspension of beads coated with blocking protein. The distribution shown in Fig. 3B indicated that the average KinExA beadpack consisted of 9980 ± 470 beads that possessed a total surface area of $263 \pm 13 \text{ mm}^2$ and occupied a total volume of $4.1 \pm 0.2 \mu\text{l}$. Since the total volume of a 4-mm-high beadpack in the observation cell is $8.0 \mu\text{l}$, the interstitial volume among the beads was $3.9 \mu\text{l}$. Thus, if the 3.9 pmol of binding sites on the surface of the beads behaved kinetically as though they were dispersed in homogeneous solution, the effective concentration of immobilized binding sites within the beadpack would be $1.0 \mu\text{M}$.

Antibody-antigen binding studies were conducted with fluorescent labels on either the primary or a secondary antibody. Having established that standard curves of binding proteins could be obtained with the KinExA, the ability of the same approach to quantify the free protein component in reaction mixtures of protein, ligand, and protein-ligand complexes was assessed in an experimental system where all of the binding partners were covalently tagged with different fluorescent molecules. The capture and retention of each component of the assay could thus be studied and quantified by simply changing the optical filter set in

the spectrofluorimeter. These experiments were devised to investigate and illustrate the principles of KinExA assays. The model binding reaction consisted of the interaction between a fluorescein-labeled anti-biotin monoclonal antibody and biotin covalently conjugated to B-phycoerythrin (5 mol of biotin/mol of protein). The immobilized ligand was biotin covalently conjugated to BSA. Following exposure of the beadpack to the reaction mixture and the removal of the unbound reagents, the amount of mouse anti-biotin captured by the immobilized ligand on the beads was also quantified by the subsequent exposure of the beadpack to an anti-species secondary antibody (goat anti-mouse) covalently coupled to Cy5.

Figure 4A shows representative examples of the time courses for the binding of primary antibody to the immobilized capture ligand when reaction mixtures consisting of a constant concentration of fluorescein-labeled anti-biotin antibody and different concentrations of biotinylated B-phycoerythrin were analyzed in the KinExA using the filter set optimized for the detection of fluorescein fluorescence. In the absence of soluble ligand (curve a), an increase in fluorescence was observed as the antibody with its unoccupied binding sites was captured by the immobilized biotinylated BSA. In the presence of a saturating concentration of soluble biotinylated B-phycoerythrin (curve e), no increase in fluorescence was observed because the binding sites on the antibody were fully occupied with the soluble ligand. In the presence of concentrations of the soluble ligand intermediate between those of zero and saturation (curves b–d), intermediate instrument responses were obtained from which the concentration of free antibody binding sites in each reaction mixture could be determined.

The secondary plot in Fig. 4B shows the dependence of the instrument response derived from the primary data on the concentration of the biotin-B-phycoerythrin conjugate. The fraction of occupied binding sites on the anti-biotin monoclonal antibody was taken as

$$\frac{\text{IR}_0 - \text{IR}_{\text{exp}}}{\text{IR}_0 - \text{IR}_{\infty}}, \quad [1]$$

where IR represents the integral of each time course such as those in Fig. 4A over the interval of 100 to 190 s, and the subscripts 0, exp, and ∞ refer to time courses corresponding to a ligand concentration of zero, an intermediate ligand concentration, and a saturating ligand concentration, respectively. A plot of the fraction of occupied binding sites on the anti-biotin antibody as a function of the concentration of biotinylated B-phycoerythrin is given in the inset of Fig. 4B. The value of the apparent dissociation constant, K_d , was

obtained from a nonlinear regression fit of the following rectangular hyperbola to the data:

Fraction of occupied binding sites

$$= \frac{[\text{biotin-B-phycoerythrin}]}{(\text{biotin-B-phycoerythrin}) + K_d} \quad [2]$$

Using the fluorescein filter set to monitor changes in the amount of fluorescein-labeled antibody captured on the beadpack, the equilibrium dissociation constant for the binding of biotinylated B-phycoerythrin to fluorescein-labeled antibody was determined to be $2.15 \pm 0.07 \times 10^{-8}$ M.

Figure 5A shows representative examples of the time courses for the fluorescence signal when the same reaction mixtures were analyzed in the KinExA using a filter set optimal for the detection of fluorescence from the biotin-B-phycoerythrin conjugate. The fluorescence signal observed in the 40- to 90-s interval was approximately proportional to the concentration of the conjugate. After the excess unbound reagents were removed from the beadpack (90–190 s), a residual fluorescence was observed that depended on the concentration of the biotinylated B-phycoerythrin in the reaction mixture. When anti-biotin was omitted from the reaction mixture, no residual fluorescence could be detected for B-phycoerythrin after the buffer wash (data not shown), indicating that nonspecific binding of the biotinylated B-phycoerythrin to the surface of the beads was negligible. It was hypothesized that the residual fluorescence arose as a consequence of the capture of bivalent anti-biotin antibodies where one of the two binding sites was occupied with a soluble biotin-B-phycoerythrin conjugate. This hypothesis was supported by the secondary plot of residual fluorescence versus the fraction of occupied binding sites on the antibody shown in Fig. 5B. The ascending portion of the curve represents reaction mixtures where either none or one of the two binding sites on the bivalent antibody is occupied with the soluble ligand. The descending portion of the curve represents reaction mixtures where either one or both of the binding sites is/are occupied with soluble ligand. For an antibody with two equal and independent binding sites, one would anticipate that the highest concentration of monoligated antibody (and the highest residual fluorescence in Fig. 5B) would occur when the ligand concentration in solution was equal to the value of the solution K_d , where the fraction of occupied binding sites would be equal to 0.5. That the peak of the curve in Fig. 5B was displaced to a value slightly lower than 0.5 is perhaps a consequence of the heterogeneous method employed by the KinExA during the capture of unliganded antibody binding sites. Thus the unoccu-

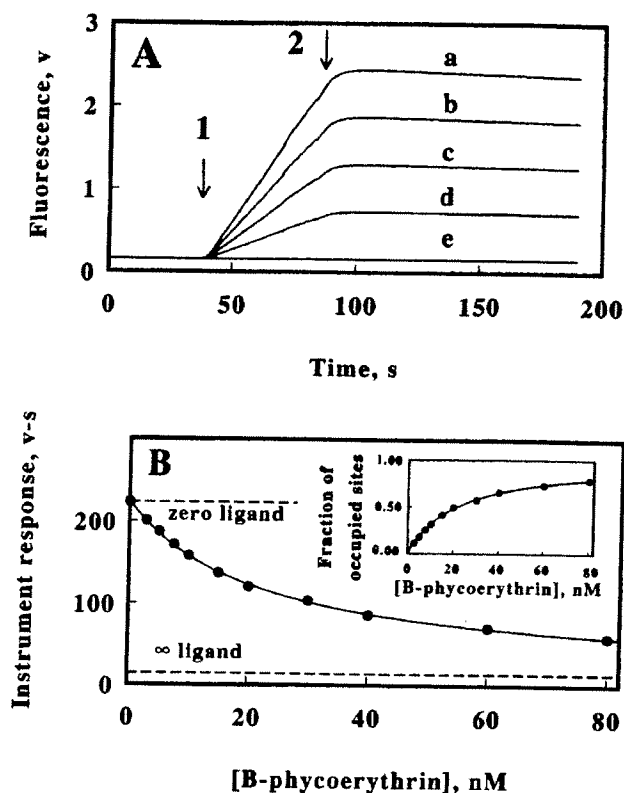


FIG. 4. Determination of equilibrium binding constants using labeled primary antibodies. (A) Time courses of fluorescence responses observed with optical filters optimal for fluorescein when beads coated with biotinylated BSA were exposed to mixtures of fluorescein-labeled mouse anti-biotin antibody and biotin covalently conjugated to B-phycoerythrin. Reagent concentrations: fluorescein-labeled mouse anti-biotin antibody, 1.0 nM (2.0 nM in binding sites); and biotin conjugated with B-phycoerythrin, 0.0, 7.6 nM, 20 nM, 50 nM, and 6 μ M in B-phycoerythrin in experiments a through e, respectively. Arrows: 1, introduction of reaction mixtures containing fluorescein-labeled mouse anti-biotin; and 2, cessation of reaction mixture and initiation of first buffer wash. (B) Secondary plot of the instrument response as a function of the total concentration of soluble biotinylated B-phycoerythrin. Instrument responses consisted of integrals of time courses (A) from 100 to 190 s. Each determination was performed in duplicate; in many cases the error in the data was less than the diameter of the plotted points. The values for the instrument responses that correspond to zero and infinite concentrations of ligand are represented by the dashed lines as indicated. Inset, the concentration of the antibody binding sites occupied by soluble antigen, determined from the secondary plot in the main panel, was expressed as a fraction of the concentration of total antibody binding sites and plotted versus the concentration of biotinylated B-phycoerythrin in solution. The parameters for the curve drawn through the data points were determined by nonlinear regression analysis using a one-site homogeneous binding model.

ried binding sites that remained on antibodies captured by the immobilized ligand during the early portions of the exposure of the reaction mixture to the beadpack would have the opportunity to bind and capture additional soluble ligand present in the remainder of the reaction mixture as it was drawn past the beads.

Figure 6A shows representative examples of the time courses for the fluorescence signal when beads that

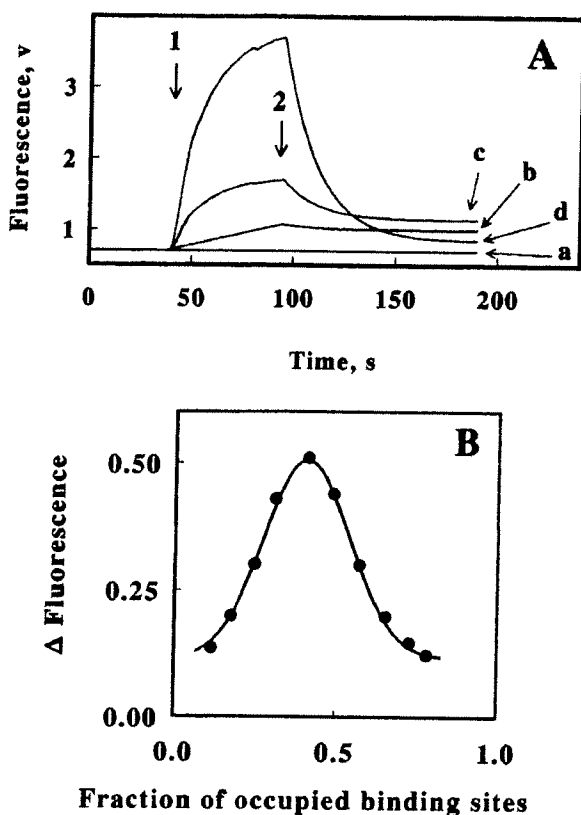


FIG. 5. Capture and retention of biotinylated B-phycoerythrin using the divalent anti-biotin monoclonal antibody and beads coated with biotinylated BSA. (A) time courses of fluorescence responses observed with optical filters optimal for B-phycoerythrin. The experimental conditions for curves a through d and the events marked by the arrows were as described in the legend for Fig. 4. (B) Dependence of the residual fluorescence on the fraction of occupied binding sites in the soluble antibody. The value of Δ fluorescence represents the average signal that remained after the first buffer wash to remove excess unbound reagents (between 185 and 190 s) minus that of the average background fluorescence from 20 to 30 s. Values of the fraction of antibody binding sites occupied by soluble antigen were taken from the inset of Fig. 4B. The parameters for the curve drawn through the data points were determined by nonlinear regression analysis using a standard Gaussian distribution function.

had been exposed to the same mixtures of fluorescein-labeled anti-biotin antibody and biotinylated B-phycoerythrin were subsequently exposed to a goat anti-mouse secondary antibody covalently labeled with Cy5 and observed using a filter set optimal for the detection of fluorescence from Cy5. When the reaction mixture contained a saturating concentration of the soluble ligand (curve e), the fluorescence approximated a square wave that corresponded to the fluorescence of the labeled secondary antibody during its transient passage past the beads in the observation cell. The signal failed to return to that of the background, indicative of a slight nonspecific binding of the secondary antibody to the beads. In the absence of soluble ligand (curve a), the fluorescence from 190 to 300 s reflected the sum of two contributions: the fluorescence of the

unbound labeled antibody in the interstitial regions among the beads, and that of the labeled secondary antibody specifically bound to the captured anti-biotin primary antibody. Binding of the labeled secondary antibody was an ongoing process that produced a positive slope in this portion of the curve. When the excess unbound label was removed from the beads with a buffer wash, the fluorescence that remained (300–400 s) was the sum of that from the nonspecifically bound antibody plus that of the labeled anti-species antibody specifically bound to the mouse anti-biotin antibody captured on the beads.

When soluble ligand was omitted and the concentration of the anti-species secondary antibody was held

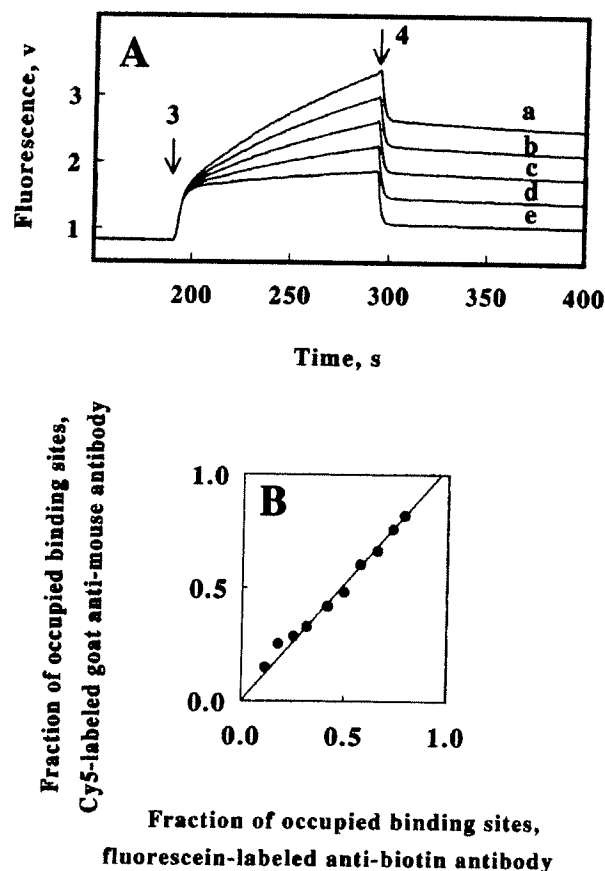


FIG. 6. Determination of equilibrium binding constants for a mouse primary antibody using a fluorescently labeled goat anti-mouse secondary antibody. (A) Time courses of fluorescence responses observed with optical filters optimal for Cy5 when beads coated with biotinylated BSA and different amounts of captured mouse anti-biotin antibody were exposed to Cy5-labeled goat anti-mouse antibodies. The experimental conditions for curves a through e were as described in the legend for Fig. 4; the concentration of Cy5-labeled polyclonal goat anti-mouse antibody was 1.0 $\mu\text{g/ml}$. Arrows: 3, introduction of Cy5-labeled goat anti-mouse antibody; and 4, cessation of labeled secondary antibody and initiation of second buffer wash. (B) Comparison of the fraction of occupied binding sites determined using labeled anti-species secondary antibodies (ordinate) with that obtained using labeled primary antibodies (abscissa). The slope of the line drawn through the data points was determined by linear regression analysis.

constant, the fluorescence signal from the secondary antibody was proportional to the concentration of the primary mouse antibody. A linear standard curve was obtained when the instrument response to the Cy5-labeled secondary antibody was plotted as a function of the concentration of primary anti-biotin antibody in reaction mixtures that lacked soluble ligand (data not shown). A secondary antibody concentration of 1.0 $\mu\text{g/ml}$ was chosen as the standard assay condition to ensure adequate signal-to-noise characteristics without the excessive consumption of Cy5-labeled protein reagent.

As was the case when the KinExA assays were analyzed using labeled primary antibody (see above), binding data for the interaction of anti-biotin with the biotin-B-phycoerythrin conjugate could also be obtained using the Cy5-labeled secondary antibodies. When reaction mixtures that contained soluble ligand at concentrations between zero and saturation were analyzed in KinExA assays that used the labeled secondary antibodies and the Cy5 filter set, a series of intermediate instrument responses was obtained (curves b–d in Fig. 6A) from which the concentration of unoccupied anti-biotin binding sites in each mixture could be determined. Data analysis using the labeled secondary antibody was strictly analogous to that described for the labeled primary antibody. The value of the equilibrium dissociation constant for the binding of biotinylated B-phycoerythrin to anti-biotin determined using labeled anti-species secondary antibodies was $2.01 \pm 0.17 \times 10^{-8} \text{ M}$, a value identical within experimental error to that determined using the fluorescein-labeled primary antibody. The close correspondence between the two data sets is illustrated by the plot in Fig. 6B. Values for the fraction of occupied binding sites in the anti-biotin antibody, as determined using the labeled secondary antibody, were plotted versus the corresponding values determined using the labeled primary anti-biotin antibody. The slope of the linear regression line drawn through the data points in the comparison was 1.03 ± 0.04 , within experimental error of the value of 1.0 anticipated for a perfect correlation.

Determination of the association and dissociation rate constants for the primary antibody–antigen interaction. To investigate the kinetics of the antigen–antibody interaction, a solution of the anti-biotin monoclonal antibody was injected into and mixed with a stream of biotinylated B-phycoerythrin that reacted for 7 s before the mixture encountered the packed beads. The primary data, which resembled those illustrated in Fig. 6A, now represented the concentration of unoccupied binding sites plucked from a mixture of binding partners that was only 7 s old and far from equilibrium. The extent of the reaction during that 7 s was controlled by varying the concentration of the re-

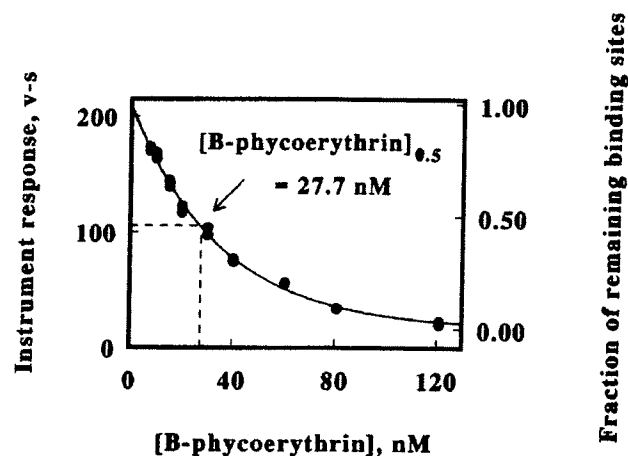


FIG. 7. Determination of the association rate constant for the bimolecular combination of mouse anti-biotin monoclonal antibody with biotin covalently coupled to B-phycoerythrin. Anti-biotin antibody (1.8 nM in binding sites) and different concentrations of biotinylated B-phycoerythrin were incubated for 7 s before separation of the primary antibodies in the mixture into bound and free fractions. Instrument responses were derived from primary data such as those shown in Fig. 6A using Cy5-labeled goat anti-mouse antibodies (1.0 $\mu\text{g/ml}$) to quantify the mouse anti-biotin antibodies that could be captured in the reaction mixture after 7 s of exposure to the soluble ligand. The curve drawn through the data points was generated using a single exponential function of the total soluble biotin concentration and a value for the bimolecular association rate constant of $3.6 \times 10^6 \text{ M}^{-1} \text{ s}^{-1}$.

agent in excess, the biotinylated B-phycoerythrin. Figure 7 shows a secondary plot of the instrument response (left ordinate) as a function of the biotin-B-phycoerythrin in the final kinetic mixture. A single exponential function of the concentration of the conjugate was fit to the data in Fig. 7:

$$\text{IR}_{[\text{biotin-B-phycoerythrin}]} = (\text{IR}_0 - \text{IR}_\infty)e^{-k_1[\text{biotin-B-phycoerythrin}]t} + \text{IR}_\infty, \quad [3]$$

where IR_0 , $\text{IR}_{[\text{biotin-B-phycoerythrin}]}$, and IR_∞ are the instrument responses at zero, intermediate, and infinitely high concentrations of the biotin-B-phycoerythrin conjugate, respectively, k_1 is the second order rate constant for the bimolecular binding of anti-biotin antibody and biotin conjugated with B-phycoerythrin, and t is 7 s. The correspondence between the experimental value of the KinExA instrument response and the calculated fraction of unoccupied binding sites that remain is illustrated by the right ordinate in Fig. 7. A value of $3.6 \pm 0.2 \times 10^6 \text{ M}^{-1} \text{ s}^{-1}$ was obtained for the bimolecular association of anti-biotin with biotinylated B-phycoerythrin from the nonlinear regression fit of Eq. [3] to the data in Fig. 7. A value for the corresponding unimolecular dissociation rate constant, $k_2 = 7.5 \times 10^{-2} \text{ s}^{-1}$, was obtained by multiplying the value of k_1 obtained from the data in Fig. 7 with the corresponding

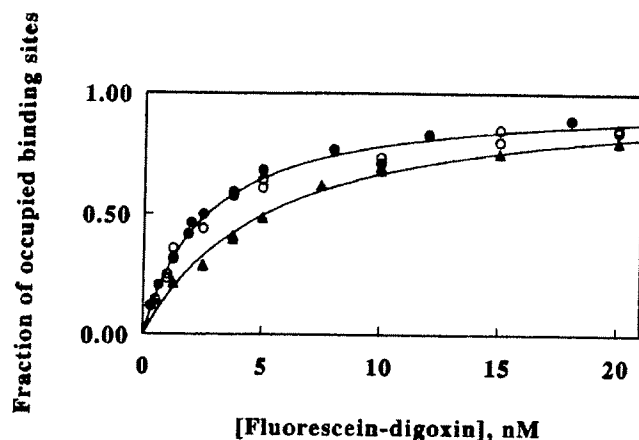


FIG. 8. Effect of protein valency on the determination of binding constants in the KinExA. Equilibrium binding curves were determined for the association of fluorescein-labeled digoxin with intact (closed triangles), $(F_{AB})_2$ (open circles), and F_{AB} (closed circles) fragments of mouse anti-digoxin antibodies. Concentrations of binding sites: intact antibodies, 0.9 nM; $(F_{AB})_2$, 1.2 nM; and F_{AB} , 1.2 nM.

value for K_d obtained from the data in Figs. 4 and 6 according to the identity $K_d = k_2/k_1$. No attempt was made to determine the unimolecular dissociation rate constant by directly monitoring the time-dependent washout of primary antibodies captured by the immobilized ligand on the beads. It was anticipated that the rebinding of newly dissociated antibody to the high concentration of immobilized ligand present on the surface of the beads would introduce too great an uncertainty into the interpretation of the dissociation data.

KinExA assays are not affected by protein binding valency. The influence of protein binding valency on the values of equilibrium dissociation constants determined by KinExA assays was assessed by preparing a monovalent F_{AB} fragment and comparing the value of K_d obtained for the fragment with that obtained for the intact bivalent antibody. The reagents for these experiments consisted of a fluorescein-labeled derivative of digoxin and a mouse monoclonal antibody directed against digoxin (clone No. 94146), a $(F_{AB})_2$ fragment of antibody 94146, and the corresponding F_{AB} fragment. The immobilized ligand was BSA covalently conjugated with digoxin; this capture ligand was adsorption coated onto standard polymethylmethacrylate beads as described for biotinylated BSA. Fluorescein-labeled goat anti-mouse antibodies were used to quantify the mouse anti-digoxin primary antibodies captured by the immobilized digoxin-BSA. KinExA assays were conducted on equilibrium reaction mixtures and the results were analyzed as described above. Figure 8 summarizes the data obtained for the binding of the soluble fluorescein-digoxin conjugate with all three forms of the antibody. Proteolytic removal of the F_C fragment and subsequent purification produced a bivalent $(F_{AB})_2$ fragment that bound to fluorescein-digoxin with

greater affinity than did the intact antibody (open circles vs closed triangles in Fig. 8). Further cleavage of the bivalent $(F_{AB})_2$ fragments into the smaller univalent F_{AB} fragments had no significant influence on the apparent affinity of the fragments for the soluble ligand (open versus closed circles in Fig. 8).

Examination of the primary KinExA traces obtained with fluorescein-digoxin and the various forms of the anti-digoxin antibody provided corroboration that the F_{AB} and $(F_{AB})_2$ fragments were truly mono- and multivalent, respectively. No residual fluorescein fluorescence was detected when beads were exposed to mixtures of F_{AB} and fluorescein-digoxin and subsequently washed to remove excess unbound reagents (data not shown). These observations confirmed that the monovalent F_{AB} fragment captured by the immobilized ligand was incapable of retaining soluble fluorescein-digoxin. In contrast, residual fluorescence was readily quantified when beads were exposed to mixtures of fluorescein-digoxin and either $(F_{AB})_2$ fragments or intact anti-digoxin antibodies. These observations confirmed that the bivalent antibody or $(F_{AB})_2$ fragment captured by the immobilized ligand possessed an additional binding site per protein for capture and/or retention of fluorescein-digoxin. Indeed, the dependence of the residual fluorescein fluorescence on the concentration of fluorescein-digoxin was identical to the analogous curve presented in Fig. 5B for the biotin-anti-biotin system (data not shown).

DISCUSSION

Unlike other automated instrumentation devoted to the study of protein binding interactions where the interaction to be quantified is that between a soluble and an immobilized binding partner, the equilibrium and kinetic rate constants determined on the KinExA are those for the binding reaction in homogeneous solution. The immobilized reactant in the KinExA is merely a tool used to separate and quantify the free proteins with unoccupied binding sites present in the solution reaction mixture. When measuring binding interactions in the KinExA, the principal conditions that must be met are: (i) binding of the immobilized and the corresponding soluble component must be mutually exclusive; and (ii) binding to the immobilized component must be sufficiently tight to permit efficient protein capture leading to an instrument response with acceptable signal-to-noise characteristics. The actual kinetic properties of binding to the immobilized reagent are immaterial as long as (i) capture from the solution phase is sufficiently rapid to generate a quantifiable signal and (ii) a constant percentage of the free protein is separated from each reaction mixture, regardless of the concentration of the competing soluble ligand. The latter condition is readily achieved by en-

sure that the effective concentration of the immobilized ligand ($\sim 1.0 \mu\text{M}$ in the example discussed above) is in a 10-fold or greater molar excess to that of the soluble protein (2.4 nM or less, above). Binding of the free protein to the immobilized ligand under these conditions is a pseudo-first-order process in which the rate and thus the extent of binding during the limited contact time between the free protein and the immobilized ligand are dictated solely by the concentration of the reagent in excess (the immobilized ligand). Under these conditions, the same percentage of free protein is bound to the immobilized ligand regardless of the absolute concentration of the soluble protein.

The method described here permits the determination of equilibrium dissociation constants over a wide range of values. The ability to quantify high affinity binding interactions is limited by two constraints regardless of the experimental approach used to quantify binding. The first is the length of time required to reach thermodynamic equilibrium in those cases where the unimolecular dissociation constants are quite small. This is a serious practical limitation in all cases, since a binding reaction where dissociation of the complex occurs with a rate constant of 10^{-5} s^{-1} will only be 87.5%, or 3 half-lives, of the way to completion after 48 h of incubation! The second constraint involves the necessity of generating a fluorescence signal sufficient for reliable quantification. This is not quite as serious a problem because free protein is accumulated and concentrated on the beads. To achieve reliable equilibrium binding data, it is necessary to ensure that the total concentration of antibody be equivalent to or less than the equilibrium dissociation constant for the binding reaction. For high affinity interactions where one must use a low concentration of the binding protein, an acceptable fluorescence signal can be obtained in the KinExA with very dilute antibodies by simply increasing the volume of the dilute equilibrium reaction mixture drawn past the beads. Our laboratories have quantified equilibrium dissociation constants in the low picomolar range using individual KinExA assays of less than 30 min each (29, and data not shown). Studies on interactions of even higher affinity become problematic due to the time required to achieve practical equilibrium in solution before analysis.

The ability to quantify low affinity binding interactions in solution is equally broad. On the one hand, the rapid dissociation of low affinity complexes means that proteins complexed with soluble ligands will dissociate and be eligible to bind to the high affinity ligand immobilized on the solid phase during the short time each portion of the sample is exposed to the beadpack. On the other hand, the high concentration of soluble ligand required to produce a given equilibrium concentration of low affinity protein–ligand complexes means that the soluble ligand can effectively compete with the

immobilized ligand by rapidly rebinding the newly dissociated protein. It is anticipated that individual components in a low affinity solution reaction mixture would remain in rapid equilibrium as small amounts of free protein were removed by the high affinity binding to immobilized ligand on the beads. The strategy that would yield the most reliable value for the bimolecular association rate constant for the solution binding reaction under these conditions is thus one where the amount of free protein captured on the beadpack was as small a portion of the total protein as possible (thus the solution reaction would be perturbed as little as possible). This could be accomplished experimentally by increasing the total protein concentration, decreasing the concentration of immobilized ligand on the beads, and/or decreasing the time of exposure to the beads (by increasing the flow rate). Our laboratories have quantified equilibrium dissociation constants in the millimolar range, although the error in the data appears to increase as the affinity decreases (data not shown).

Values for the bimolecular association rate constants of high affinity interactions are also readily determined in the KinExA by adjusting the concentration of the soluble ligand in the injection experiments described above such that the secondary data describe the greater part of an exponential curve such as the one shown in Fig. 7. Our laboratories have quantified second-order association rate constants in excess of $10^7 \text{ M}^{-1} \text{ s}^{-1}$ (30, and data not shown). One limitation of this method is its inability to quantify bimolecular association rate constants for low affinity binding interactions, due to the finite time required to transport the newly mixed binding reagents from the point of mixing to the beadpack. The difficulty in studying the kinetics of low affinity interactions is that the combination of high unimolecular dissociation rate constants and the high concentrations of soluble ligand necessary to form protein–ligand complexes dictate that equilibrium is achieved in solution reaction mixtures well within the 7 s it takes the newly formed mixture to encounter the beadpack. Thus, this method is not generally amenable to kinetic studies on binding reactions with unimolecular dissociation rate constants of 1.0 s^{-1} or higher (corresponding roughly to equilibrium dissociation constants on the order of $1.0 \mu\text{M}$ or higher for reactions with association rate constants on or around $10^6 \text{ M}^{-1} \text{ s}^{-1}$). In principle, one could extend the range of binding reactions amenable to kinetic studies by moving the observation cell closer to the point of mixing and by increasing the flow rate over the beadpack, although the latter change is of limited utility because it would also serve to decrease the magnitude of the fluorescence signal. It is unlikely that these proposed changes in the current configuration of the KinExA instrument would extend the range of dissociation constants

amenable to kinetic studies by more than a single order of magnitude.

The concentration of free protein present in equilibrium reaction mixtures can also be determined using other instrumentation devoted to protein binding studies. For example, a "free capture mode" was described using the Threshold immunoassay system that is strictly analogous to the heterogeneous method described here (31, 32). The Threshold system uses a membrane derivatized with biotin or complexes of biotin and streptavidin to filter, capture, and concentrate one of the free, unbound components in each reaction mixture. The subsequent detection step consists of the deposition of urease activity within the membrane that is proportional to the amount of solution reagent captured, followed by the quantification of urease-dependent changes in solution pH that are measured with a light-addressable potentiometric sensor. The weakness of this system is that one or both of the participating solution reagents must be covalently coupled with either a small molecule (biotin or fluorescein) or a macromolecule (streptavidin or urease). Thus the binding reaction that is conducted in homogeneous solution must be performed with covalently derivatized reagents that may not exhibit the same properties as the native reagents. Heterogeneous competition experiments were also described using instruments based on SPR detection methods (33–37). Pluckthun *et al.* (38) described a heterogeneous assay similar to that presented here except that a BIAcore instrument was used to quantify the concentration of free proteins with unoccupied binding sites. The principal limitation using the BIAcore was the lower sensitivity compared to other instrumentation; a minimal total antibody concentration of 50 nM was required to obtain acceptable signals when the free antibody was determined from association rate data in the BIAcore (38). Since the most reliable values for equilibrium dissociation constants are obtained when the protein concentration is less than or equal to the value of the K_d , the low sensitivity of the BIAcore compared to other instruments clearly limits the scope and range of binding reactions that can be studied by this competition method using SPR. Two other limitations of the Threshold and SPR systems should be noted. First, the possible effects of protein multivalency upon the values of equilibrium binding constants determined with either system have been discussed (31, 38), but remain unresolved experimentally. Multivalency of protein binding reactions was not an issue in KinExA assays (Fig. 8). Second, neither the Threshold nor the BIAcore is mechanically equipped to conduct kinetic studies by the heterogeneous method described above for the rate data presented in Fig. 7. Currently, only the KinExA has an injection mode that permits reasonably short-lived reaction mixtures to be analyzed.

The experiments described herein, where all of the principal reagents were covalently conjugated with different fluorescent molecules, were conducted to investigate and illustrate the principles of KinExA assays. During the routine determination of equilibrium or kinetic binding constants for other protein–ligand combinations, only the secondary antibody needs to be covalently labeled with a fluorescent molecule. That is, the binding reaction that occurs in homogeneous solution can be conducted with native, underivatized molecules. When the primary binding reaction in solution is that between an antibody and an antigen, these KinExA assays are very convenient because anti-species secondary antibodies labeled with a variety of fluorescent molecules are available from many commercial sources. We have found the KinExA to be a remarkably sensitive tool for the characterization of antibody–antigen interactions. As part of a functional characterization of a monoclonal antibody directed against chelated ionic cadmium, our laboratories determined 25 individual equilibrium and rate constants while consuming less than 500 μ g of purified antibody (30). Typical assay conditions that employed 0.5 nM antibody generated fluorescence signals of around 1.0 V with 1 to 2 mV noise. Further, the cost of disposable reagents was minimal compared with other heterogeneous methods of measuring binding. It is hoped that these KinExA assays will enjoy widespread use in the efforts of life scientists to understand complex biochemical processes at the molecular level.

ACKNOWLEDGMENTS

We thank Steve Lackie for many fruitful discussions and a critical reading of the manuscript. This work was supported by Grants DE-FG02-96ER20228 and GM08008-26S1 from the U.S. Department of Energy and the National Institutes of Health, respectively, and Grant DSWA01-97-1-0028 from the Defense Special Weapons Agency of the U.S. Department of Defense to the Tulane–Xavier Center for Bioenvironmental Research.

REFERENCES

1. Edsall, J. T., and Wyman, J. (1958) *Biophysical Chemistry*, Vol. 1, Academic Press, New York.
2. Steinhardt, J., and Reynolds, J. A. (1969) *Multiple Equilibria in Proteins*, Academic Press, New York.
3. Weber, G. (1975) *Adv. Protein Chem.* **29**, 1–83.
4. Connors, K. A. (1987) *Binding Constants: The Measurement of Molecular Complex Stability*, Wiley, New York.
5. Phizicky, E. M., and Fields, S. (1995) *Microbiol. Rev.* **59**, 94–123.
6. Friguet, B., Chaffotte, A. F., Djavadi-Ohanian, L., and Goldberg, M. (1985) *J. Immunol. Methods* **77**, 305–319.
7. Carter, R. M., Jacobs, M. B., Lubrano, G. J., and Gilbault, G. G. (1995) *Anal. Lett.* **28**, 1379–1386.
8. Arnold, M. A. (1992) *Immunochemical Assays and Biosensor Technology for the 1990s* (Nakamura, R. M., Kasahara, Y., and Rechnitz, G. A., Eds.), pp. 311–333. Am. Chem. Soc., Washington, DC.

9. Chaiken, I., Rose, S., and Karlsson, R. (1992) *Anal. Biochem.* **201**, 197–210.
10. Karlsson, R., Michaelsson, A., and Mattsson, L. (1991) *J. Immunol. Methods* **145**, 229–238.
11. Jonsson, V., and Malmqvist, M. (1992) *Adv. Biosensors* **2**, 291–336.
12. Schuck, P. (1997) *Annu. Rev. Biophys. Biomol. Struct.* **26**, 541–566.
13. Schuck, P. (1996) *Biophys. J.* **70**, 1230–1249.
14. Schuck, P., and Minton, A. P. (1996) *Anal. Biochem.* **240**, 262–272.
15. Glaser, R. W. (1993) *Anal. Biochem.* **213**, 152–161.
16. O'Shannessy, D. J. (1994) *Curr. Opin. Biotechnol.* **5**, 65–71.
17. O'Shannessy, D. J., and Winzor, D. J. (1996) *Anal. Biochem.* **236**, 275–283.
18. Mach, H., Volkin, D. B., Burke, C. J., Middaugh, C. R., Linhardt, R. J., Fromm, J. R., Loganathan, D., and Mattsson, L. (1993) *Biochemistry* **32**, 5480–5489.
19. Edwards, P. R., Gill, A., Pollard-Knight, D. V., Hoare, M., and Buckle, P. E. (1995) *Anal. Biochem.* **231**, 210–217.
20. Schuck, P., and Minton, A. P. (1996) *Trends Biochem. Sci.* **21**, 458–460.
21. Karlsson, R., Roos, H., Fagerstam, L., and Persson, B. (1994) *Methods: Companion Methods Enzymol.* **6**, 99–110.
22. Yeung, D., Gill, A., Maule, C. H., and Davies, R. J. (1995) *Trends Anal. Chem.* **14**, 49–56.
23. Ito, W., and Kurosawa, Y. (1993) *J. Biol. Chem.* **268**, 20668–20675.
24. Bondeson, K., Frostell-Karlsson, A., Fagerstam, L., and Magnusson, G. (1993) *Anal. Biochem.* **214**, 245–251.
25. Guichard, G., Benkirane, N., Zeder-Lutz, G., Van Regenmortel, M. H. V., Briand, J. P., and Muller, S. (1994) *Proc. Natl. Acad. Sci. USA* **91**, 9765–9769.
26. Kalinin, N. L., Ward, L. D., and Winzor, D. J. (1995) *Anal. Biochem.* **228**, 238–244.
27. MacKenzie, C. R., Hiram, T., Deng, S. J., Bundle, D. R., and Narang, S. A. (1996) *J. Biol. Chem.* **271**, 1527–1533.
28. O'Shannessy, D. J., Brigham-Burke, M., Soneson, K. K., Hensley, P., and Brooks, I. (1994) *Methods Enzymol.* **240**, 323–349.
29. Kaplan, B. E., Hefta, L. J., Blake, II, R. C., Swiderek, K. M., and Shively, J. E. (1998) *J. Peptide Res.* **52**, 249–260.
30. Blake, D. A., Chakrabarti, P., Khosraviani, M., Hatcher, F. M., Westhoff, C. M., Goebel, P., Wylie, D. E., and Blake, II, R. C. (1996) *J. Biol. Chem.* **271**, 27677–27685.
31. Dill, K., Lin, M., Poteras, C., Fraser, C., Hafeman, D. G., Owicki, J. C., and Olson, J. D. (1994) *Anal. Biochem.* **217**, 128–138.
32. Panfili, P. R., Dill, K., and Olson, J. D. (1994) *Curr. Opin. Biotechnol.* **5**, 60–64.
33. Karlsson, R. (1994) *Anal. Biochem.* **221**, 142–151.
34. Hall, D. R., and Winzor, D. J. (1997) *Anal. Biochem.* **244**, 152–160.
35. Karlsson, R., Jendeberg, L., Nilsson, B., Nilsson, J., and Nygren, P. A. (1995) *J. Immunol. Methods* **183**, 43–49.
36. Morelock, M. M., Ingraham, R. H., Betageri, R., and Jakes, S. (1995) *J. Med. Chem.* **38**, 1309–1318.
37. Ward, L. D., Howlett, G. J., Hammacher, A., Weinstock, J., and Yasukawa, K. (1995) *Biochemistry* **34**, 2901–2907.
38. Nieba, L., Krebber, A., and Pluckthun, A. (1996) *Anal. Biochem.* **234**, 155–165.